



Purifying surface waters contaminated with natural organic matters and bacteria using Ag/PDA-coated PES membranes

Kok Poh Wai¹, Chai Hoon Koo^{2,†}, Yean Ling Pang¹, Woon Chan Chong¹, Woei Jye Lau³

¹Department of Chemical Engineering, Lee Kong Chian Faculty of Engineering and Science, Universiti Tunku Abdul Rahman, Bandar Sungai Long, Cheras, 43000 Kajang, Selangor, Malaysia.

²Department of Civil Engineering, Lee Kong Chian Faculty of Engineering and Science, Universiti Tunku Abdul Rahman, Bandar Sungai Long, Cheras, 43000 Kajang, Selangor, Malaysia.

³Advanced Membrane Technology Research Centre (AMTEC), School of Chemical and Energy Engineering, Universiti Teknologi Malaysia, 81310 Skudai, Johor, Malaysia.

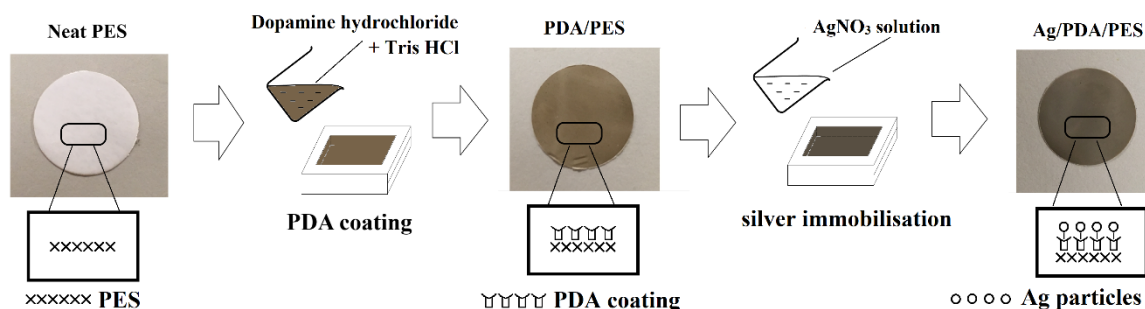
Received February 28, 2022 Revised November 03, 2022 Accepted February 08, 2023

ABSTRACT

Polymeric membrane is susceptible to fouling particularly when it is used to treat surface water contaminated by natural organic matters and bacteria. Surface modification may address the issue by imparting antifouling and antibacterial properties to the membrane. In this study, a neat polyethersulfone (PES) membrane (denoted as membrane P1) was prepared by phase inversion method followed by polydopamine (PDA) coating to improve its membrane hydrophilicity. Thereafter, the physicochemical properties of the PDA-coated PES membrane (denoted as membrane P3) were further improved by in situ reduction of silver (Ag) onto its surface to impart antibacterial properties (denoted as membrane P4). All membranes were instrumentally characterized while their filtration performance against humic acid (HA) and antibacterial properties were evaluated. Results showed that membrane P1 removed 77.81% of HA and achieved a fouling recovery rate (FRR) of 65.72%. Upon Ag immobilization, the HA rejection of membrane P4 was further improved to 95.14% with FRR recorded at 92.17%. This membrane also demonstrated good stability and excellent antibacterial properties over other fabricated membranes (P1, P2 and P3) in this study. Moreover, it exhibited a lower total flux decline and higher contaminant removal performance over membrane P1 in treating surface water samples.

Keywords: Antifouling, Enhanced hydrophilicity, Flux recovery rate, Real sample, Silver immobilization

Graphical Abstract



This is an Open Access article distributed under the terms of the Creative Commons Attribution Non-Commercial License (<http://creativecommons.org/licenses/by-nc/3.0/>) which permits unrestricted non-commercial use, distribution, and reproduction in any medium, provided the original work is properly cited.

† Corresponding author
E-mail: kooch@utar.edu.my
Tel: +603-90860288 Fax: +603-90198868
ORCID: 0000-0001-7287-3394

1. Introduction

Water stress is among the main problems that currently being faced by many societies in the twenty-first century [1]. The presence of organic pollutants in water sources severely deteriorates its quality and limits its usage. These pollutants consume oxygen (to decay) and thus lower available oxygen in the water, affecting the organisms living in the stream. The breakdown of plant and animal tissues releases a mixture of carbon-based compounds, known as natural organic matters (NOMs) which potentially contribute towards water contamination. Apart from reacting with chlorine to form carcinogenic compounds, NOMs also cause unpleasant taste and colour in the water body. Therefore, humic acid (HA) as the major species in NOMs was widely used to study separation efficiency and antifouling capability of pressure-driven membranes [2,3].

Different methods of removing NOMs from water source have been reported in the literature including coagulation, advanced oxidation processes, adsorption and so forth [4–6]. Membrane process that operates as a stand-alone filtration unit possesses several advantages over other methods such as a small footprint, low manpower requirement and easy as well as flexible operation with minimal use of chemicals [7]. The polyethersulfone (PES) is a frequently used polymer for ultrafiltration (UF) membrane fabrication particularly in removing NOM [8–10]. Despite the PES membrane possessing good mechanical properties, thermal stability and chemical inertness, the neat PES membrane has a moderately high water contact angle, which indicates its hydrophobic nature and susceptibility to fouling [10–12]. On top of that, the filtration of surface water containing organic compounds along with the bacteria population using a hydrophobic membrane would easily give rise to membrane biofouling that is difficult to be removed and would cause a sharp decline in flux and membrane lifespan [11]. To prevent the membranes from losing their inherent characteristics and performance due to biofouling, the membrane surface properties must be carefully tailored using innovative approaches.

Previous studies had proven that the coating of hydrophilic polymers on the membrane surface could tackle membrane fouling effectively because a hydrophilic surface could prevent the deposition of hydrophobic foulants [13]. Amongst various modifiers, bioinspired polydopamine (PDA) emerges as a promising material to fit the purpose. The high anchoring ability of PDA film can anchor metal nanoparticles via a chemical reaction of immobilization and offer secondary functionalization [11]. Furthermore, the PDA possesses many advantages such as self-polymerization, compact structure and special recognition [14]. The hydrophilic functional groups in the PDA film would decrease static water contact angle and improve membrane wettability against the adsorption of hydrophobic foulants [15,16]. On the other hand, silver (Ag) has been reported as an excellent antimicrobial agent regardless of its state [15,17,18]. Studies showed that direct interaction between Ag and *Escherichia coli* (*E. coli*) would form holes and pits on the bacterial cell wall, causing cytoplasmic material to leak out and eventually lose its morphological integrity [15,19]. Upon entering the bacterial cell, the released Ag⁺ ions would

bind to deoxyribonucleic acid (DNA) bases to prevent DNA replication as well as cell division [15,20,21]. The exact toxicity mechanism of Ag remains debatable but most researchers opined that both metallic Ag⁰ and the released Ag⁺ ions contribute to antibacterial properties. Various approaches have been adopted to incorporate Ag into the polymeric membrane. Among others, *in situ* immobilization of Ag would be a preferred route to ensure Ag deposition on the membrane surface for maximum biocidal capacity. With a high reductive ability with a redox potential of -795 mV, the catechol groups in PDA would oxidize to catechoquinone while the chelated Ag⁺ ions will be reduced into Ag⁰ almost instantaneously [9,13]. The reduced Ag⁰ would be strongly anchored on the PDA film, for which the stable adhesion will control the release of Ag in the filtration process [13,22].

Surface immobilization of Ag on PDA has been adopted in several fields including biomedical applications [23,24] and membrane technology. Wang *et al.* [22] incorporated Ag into the PDA-coated polyacrylonitrile (PAN) membrane and applied it in the emergency water treatment system. However, the author did not study foulant rejection or membrane antifouling behaviour. In contrast, Huang *et al.* [15] synthesized Ag/PDA on a commercial polysulfone (PSf) membrane for bovine serum albumin (BSA) rejection. In the biofouling experiment, the Ag/PDA/PSf membrane reported a lower flux decline at 17% compared to a control PSf membrane at 45%. Significant enhancement in membrane wettability can be noticed alongside with a slight improvement in solute rejection from 80 to 85% upon Ag/PDA modification. Nevertheless, the modified membrane has improved anti-adhesive property and showed a higher sterilization ratio at 91% upon 30 min contact with *E. coli* cells. In a recent study, Saraswathi and co-workers [13] fabricated Ag/PDA supported poly(ether imide) (PEI) membrane for the removal of BSA protein, oil and HA aqueous solution. Hydrophilicity enhancement contributed by PDA coating and Ag immobilization increased rejection performance and flux recovery rate (FRR) by approximately 20% against all three types of foulant. The authors also reported the synthesized Ag/PDA/PEI membrane demonstrated excellent antibacterial properties in the diffusion inhibition zone test.

To our best knowledge, the study involving Ag/PDA-modified membranes in treating surface water was rarely reported. Most studies only focused on synthetic foulants like BSA, oil and organic dye instead of the actual water sample. Many types of pollutants exist in surface water samples (*i.e.* river water samples), thus the Ag/PDA-modified membrane could behave differently in terms of solute rejection as well as antifouling properties. Moreover, the filtration of surface water samples containing different types of microorganisms may give rise to complex fouling issues and lower bacterial removal performance. The results of the bacterial diffusion inhibition zone test would not be sufficient to justify the bacteria removal efficiency of the fabricated membrane. Hence, the performance of Ag/PDA-modified membranes in treating surface water samples must be carefully investigated to ensure their practicability. The River of Life Project was launched by the Malaysia Government to restore Klang River along Kuala Lumpur Independence Square for recreational use. Water fountains, pools and water mist systems that create atmospheric fog effects were built with light shows, which turn the waterfront landmark into

a stunning cobalt blue at night. In such circumstances, water reclamation from the Klang River for landscaping purposes is, therefore, a socially and environmentally viable solution. This effort could help to utilize our water resources more efficiently and reduce the stress of water scarcity especially during the dry season. The paramount factor of enabling a cost-effective water reclamation system in the city centre through membrane technology is its small footprint and relatively simpler operation with minimal chemicals.

In the current study, the rejection performance and antifouling properties of different types of membranes (i.e., PES, PES+PVP, PDA/PES+PVP and Ag/PDA/PES+PVP) were first compared using a synthetic feed solution containing HA. The membrane antimicrobial activity was evaluated using an electron microscope and bacterial disk diffusion assay. The cross-sectional and surface of the fabricated membranes were viewed under a scanning electron microscope (SEM) and field emission scanning electron microscope (FESEM), respectively. The elemental composition of the membranes was quantified by energy-dispersive X-ray analysis (EDX) whereas the membrane wettability was studied using a static water contact angle goniometer. The stability of the immobilized Ag on membrane P4 (Ag/PDA/PES+PVP) was investigated using inductively coupled plasma-optical emission spectrometry (ICP-OES). This membrane was further adopted in treating two types of surface water samples, namely Kelana Lake and Klang River water samples and their performances were then compared with the control PES membrane to outline the improvements granted by PDA coating and Ag immobilization.

2. Experimental

2.1. Materials

Polyethersulfone (PES, pellet, 35 kDa) was received from Solvay, United Kingdom (UK) while polyvinylpyrrolidone (PVP, powder, 29 kDa) was purchased from Sigma-Aldrich, Germany. N-methyl-2-pyrrolidone (NMP, > 99.5%) was obtained from Merck, Germany. Dopamine hydrochloride (powder, > 99%) and Trizma-HCl buffer solution (Tris-HCl, 1M) were obtained from Sigma-Aldrich, Germany. Silver nitrate solution (2.5 w/v% AgNO₃ in H₂O) and humic acid (HA, powder, 4.71 kDa) were supplied by Sigma-Aldrich, Switzerland. Sodium bicarbonate (pellet, > 99%) was provided by Chemsoln, Malaysia. All analytical reagents were used as received. The distilled water adopted in the experiment was produced by a laboratory water distiller (W4L Water Stills) supplied by Favorit, Malaysia.

2.2. Membrane Preparation

All PES membranes were synthesized by phase inversion technique. First and foremost, the polymers (PES and PVP) were dried at 60 °C oven (Mermert, Germany) for 12 h. To fabricate the control membrane (designated as P1), 25 wt% PES was added into solvent NMP and stirred overnight at 50 °C [25]. Other membranes, i.e., P2, P3 and P4 (see Table S1) were fabricated under a similar stirring condition but with the addition of 6 wt% of

PVP as a pore-forming agent. The dope solutions were left to cool at room temperature for 30 min before casting the membrane using an adjustable doctor blade (Braive Instrument, Germany) at the rate of 5 cm / min in an atmosphere of 90% relative humidity [26]. The wet polymeric film was then immersed in a 25 ± 2 °C distilled water coagulation bath [10]. The membrane was formed and kept in 300 mL deionized water before modification and performance evaluation. The composition of dopes and the surface modifications of the membranes are tabulated in Table S1.

2.3. Membrane Modification

The PES+PVP membrane (membrane P2) was secured on the custom-made acrylic plate with its active surface exposed to 2 g/L of dopamine solution in 0.05 M Tris-HCl buffer for 4 h. The dopamine monomers would oxidize gradually in the presence of oxygen and change the membrane surface colour from white to dark brown. To get rid of the loosely adhered PDA, the membrane samples were rinsed off with distilled water and stored wet before use. This membrane was then denoted as membrane P3 (PDA/PES+PVP). For Ag immobilization, the PDA/PES+PVP membrane was fixed on the acrylic plate again with its active surface exposed to 1 g/L AgNO₃ solution (in deionized water) for 2 h. The Ag⁺ ions would be reduced to Ag⁰, immobilized on the PDA film and changed the membrane surface colour to silvery-grey. This Ag/PDA/PES+PVP membrane (membrane P4) was then rinsed with distilled water to remove loosely immobilized Ag⁰ and stored wet. Fig. S1 illustrates the approach employed to modify the surface properties of the membrane.

2.4. Membrane Characterization

The cross-sectional and surface of the fabricated membranes were viewed under a scanning electron microscope (SEM, Hitachi S-3400N, Japan) and field emission scanning electron microscope (FESEM, JOEL JSM-6701F, Japan), respectively. The membrane samples were cracked in cryogenic liquid nitrogen and sputtered with gold before cross-sectional SEM analysis. The elemental composition of the fabricated membranes was quantified using energy-dispersive X-ray analysis (EDX, Ametek Apollo X, USA). The static water contact angle of the membranes was determined by using a contact angle goniometer (CA, Krüss GmbH, Germany). 2 µL of deionized water was dropped on each surface of the membrane specimens and the static water contact angle was measured after five seconds. The measurement was repeated at three different locations in each membrane sample and the values were averaged to obtain a mean value.

2.5. Membrane Performance Evaluation

2.5.1. Pure water permeability test

The pure water permeability (PWP) test was performed at 1 bar using a Sterlitech™ HP 4750 dead-end cell with an effective membrane area of 14.6 cm². All membrane specimens were compacted at 2 bar for 30 min before the experiment. The water permeation flux, J_w of the membrane specimen was determined using Eq. (1) [14,15],

$$J_w = \frac{V}{A \times t} \quad (1)$$

where V is the volume of permeate produced (L), A represents the effective membrane area (m^2) and t is the sampling duration (h). The membrane PWP was obtained as Eq. (2) [10,12],

$$PWP = \frac{J_w}{\Delta p} \quad (2)$$

where Δp is the operating pressure (bar). The PWP test was repeated three times for each membrane sample and the readings were averaged to a mean value.

2.5.2. Humic acid rejection and antifouling tests

The HA rejection test was performed in a Sterlitech™ HP 4750 dead-end cell using 10 ppm of HA solution. During the filtration process at 1 bar, the feed solution was continuously stirred at 300 rpm to minimize concentration polarization. The permeate was poured into a quartz cuvette and its UV absorbance at 254 nm was recorded by using UV-vis spectrophotometer (PG instrument, T60U, UK) [12]. A pre-drawn standard calibration curve was adopted to determine HA concentration before the rejection was computed using Eq. (3) [10,12,13],

$$R_{HA} = \left(1 - \frac{C_p}{C_f}\right) \times 100 \quad (3)$$

where R_{HA} indicates the HA rejection percentage whereas C_p and C_f represent HA concentration of permeate and feed, respectively. The membranes' antifouling properties were compared according to their flux recovery rate (FRR, %), in which a higher FRR value signifies a better antifouling characteristic of the membrane. The initial water flux, J_{w1} ($\text{L}\cdot\text{m}^{-2}\cdot\text{h}^{-1}$) of the fresh membrane was determined by using Eq. (1). Typically, 200 mL of 10 ppm HA was filtered across the membrane sample and discarded. The fouled membrane was held using a pair of forceps and the active surface was rinsed with running distilled water for 10 min. Next, the water flux of the regenerated membrane was determined using the same operating pressure and recorded as J_{w2} ($\text{L}\cdot\text{m}^{-2}\cdot\text{h}^{-1}$). The FRR could be treated as a suitable index of antifouling characteristics and computed as Eq. (4) [27–29].

$$\text{FRR} = \left(\frac{J_{w2}}{J_{w1}}\right) \times 100 \quad (4)$$

where J_{w1} and J_{w2} represent the pure water flux of the membrane before and after HA filtration, respectively. The HA rejection and FRR tests were repeated three times for each membrane sample and the readings were averaged to a mean value.

2.5.3. Membrane antibacterial activity

The bacteriostatic action of the fabricated membrane was demonstrated in a diffusion inhibition zone test. 100 μL of *E. coli* inoculum (3.0×10^8 CFU/mL) was spread evenly on a petri dish containing sterilized agar. A membrane disk of 15 mm diameter was deposited on the sterilized agar and incubated at 37 °C for 24 h. The bacteria

inhibition zone was observed and the diameter was measured to examine the membrane bacteriostatic effect.

To illustrate the bactericidal capability, the fabricated membranes were chopped into a 5 mm diameter membrane disc, irradiated by UV and placed on the sterilized agar. Exactly 50 μL of 3.0×10^8 CFU/mL of *E. coli* suspension was carefully dropped on the membrane surface and the agar plate was incubated at 37 °C for 24 h before SEM observation.

2.5.4. Long-term stability test of Membrane P4

The stability of immobilized Ag was assessed based on the Ag concentration detected in the permeate. Deionized water was filtered across membrane P4 for 48 h at 1 bar. The permeate was collected every 6 h and the concentration of Ag was quantified using ICP-OES (PerkinElmer Optima 7000DV, USA).

2.6. Performance Evaluation of Membrane P4 Using Surface Water Samples

Membrane P4 (Ag/PDA/PES+PVP) which carried the highest rejection and antibacterial properties was adopted to treat surface water samples. Its performance was compared with the control membrane (P1) to identify how much performance enhancement was granted upon membrane modification by PDA coating and silver immobilization. The lake and river water samples from Kelana Lake (3°05'36.4" N, 101°35'51.3" E) and Klang River (3°08'50.6" N, 101°41'42.6" E) were collected on a sunny morning and followed by storage in a refrigerator at 4 °C.

2.6.1. Total flux decline (TFD)

250 mL of distilled water was filtered across the membrane samples in a dead-end cell at 1 bar and the water flux was recorded as J_{w1} . Then, 250 mL of the surface water sample was filtered across the membranes at the same operating pressure and the permeate flux was recorded as J_p . The percentage of total flux decline was calculated using Eq. (5) [30].

$$\text{Total Flux Decline (\%)} = \left(1 - \frac{J_p}{J_{w1}}\right) \times 100 \quad (5)$$

where J_{w1} and J_p represent the initial water flux and permeate flux of the surface water sample ($\text{L}\cdot\text{m}^{-2}\cdot\text{h}^{-1}$), respectively. The TFD test was repeated three times for each membrane sample and the readings were averaged to a mean value.

2.6.2. Water samples quality assessment

The quality of the lake and river water samples before and after filtration using membranes P1 and P4 were analyzed using various analytic methods, including total suspended solids (TSS), turbidity, chemical oxygen demand (COD), total dissolved solids (TDS) and pH. The TSS of the water samples was determined based on APHA Standard Methods 2540D while the turbidity of water samples was measured using a turbidimeter (Eutech Instruments, TN-100, Singapore). By employing the HACH Standard Method 8000 for Low Range COD and digestion technique, the COD value of the water samples was determined using a spectrophotometer (HACH, DR3900, USA). The TDS value of water samples was measured using a benchtop conductivity/TDS meter (Jenway, Model 4510,

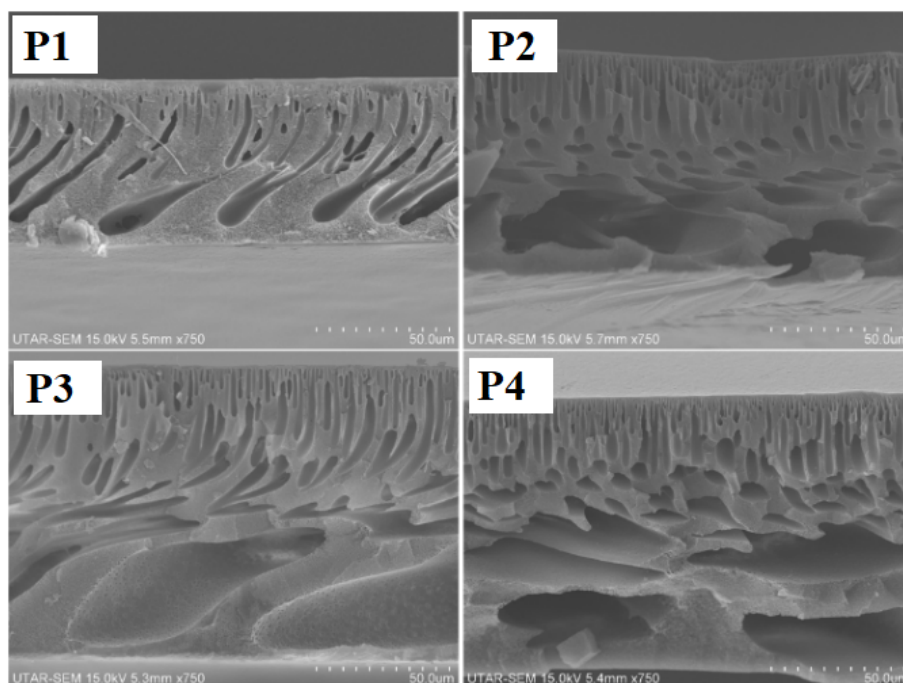


Fig. 1. Cross-sectional morphologies of membranes.

UK) while the pH value was measured using a portable pH meter (Mettler Toledo, LP115 pH meter, USA). The water sample quality assessment test was repeated three times for each membrane sample and the readings were averaged to a mean value.

2.6.3. Removal of bacterial from Klang River and Kelana Lake water by filtration

The bacterial removal performance by filtration between membranes P1 and P4 was compared using lake and river water samples. 200 mL of water sample was filtered across both membranes (P1 and P4) at 1 bar in the sterilized dead-end cell. Spread plate count was conducted on the permeate based on APHA Standard Methods 9215C. A dilution factor of $10\times$ was applied before $200\ \mu\text{L}$ of the sample was spread on the sterilized agar. The agar plates were sealed with parafilm and incubated at 37°C for 48 h. The number of bacteria colonies formed on the agar plate was observed and recorded.

3. Results And Discussion

3.1. Membrane Characterization

3.1.1. Cross-sectional morphologies

The SEM images in Fig. 1 demonstrate the cross-sectional membrane morphologies at $750\times$. As can be seen, the fabricated membranes displayed an asymmetric structure with a finger-like top sublayer connected to a bottom sublayer containing macrovoids. Membrane P1 is very dense and packed while the pore channels in the top sublayer were blocked probably due to a delayed demixing process [31]. Thus, membrane P1 was forecasted to have lower

water permeability and separation efficiency. For membrane P2, a thicker skin layer and evenly distributed pore channels could be observed. The hydrophilic PVP induced thermodynamic instability in the casting solution to speed up the demixing process and formed larger macrovoids in the porous bottom sublayer [32]. The finger-like structure of the membranes P2, P3 and P4 are well distributed as compared to that of membrane P1 (pure PES). Hence, it was believed that the former membranes would exhibit better rejection performance than the latter. On top of that, no significant difference in bulk morphology among membranes P2, P3 and P4 can be visually noticed. This is because the modification was only carried out on the surface of the resultant membrane without altering the bulk structure of cross-section.

3.1.2. Surface morphologies

The FESEM images in Fig. 2 illustrate the membranes' surface morphologies at $10,000\times$. Membrane P1 displays irregular pore sizes on the surface with several huge pores, which probably accounts for poor rejection. By blending 6% of PVP into membrane P2, the pore agent regulated pores formation, minimizing the range of pore sizes but increasing the surface pore density. By having diminished pore sizes and the absence of huge pores, membrane P2 is expected to show higher separation efficiency.

During membrane modification, the dopamine monomers oxidized on the membrane surface via multiple interactions such as covalent bonding, hydrogen bonding and p-p stacking [9]. A continuous PDA film was formed on the membrane surface accompanied by several PDA aggregates due to the accumulation and conjugation of the PDA nanoaggregate. Hence, the PDA film covered up the surface pores and renders it invisible under the electron microscope. Upon Ag immobilization, silvery-grey particles were

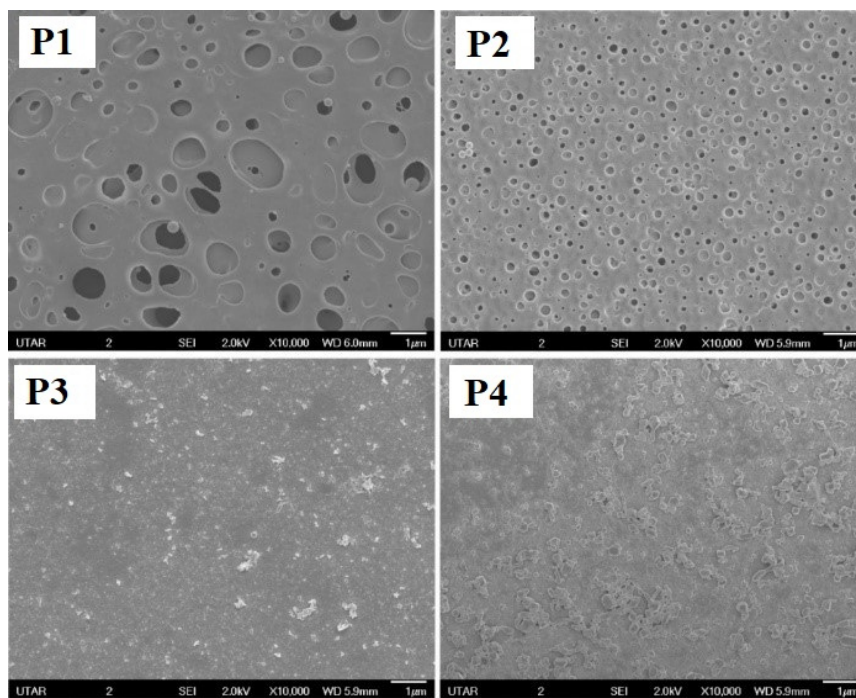


Fig. 2. Surface morphologies of membranes.

found on membrane P4. A slight agglomeration can also be observed due to the copious loading of Ag that blocked the membrane surface. This phenomenon is expected to negatively affect membrane permeation [9].

3.1.3. Membrane elemental composition

The elemental composition of membranes is presented in Table S2. As membrane P1 was made up of solely PES molecules, only carbon (C), oxygen (O) and sulphur (S) composition were displayed. The addition of 6 wt% PVP into membrane P2 shows a minor composition of nitrogen (N) in the EDX spectrum. As the PVP molecules have a greater affinity towards coagulant (water) as compared to solvent (NMP), the PVP molecules leached out from the casting film during the demixing process [33,34]. Upon PDA coating, the N composition of membranes P3 and P4 was reported in the range of 4-5% probably due to the presence of amine functional groups in the PDA coating. The additional Ag element detected in the EDX analysis also justified the successfully immobilized Ag on membrane P4.

3.1.4. Static water contact angle

Static water contact angle measurement was performed and the membrane P1 that made of semi-hydrophobic PES material exhibited a contact angle of $73.73^\circ \pm 0.61^\circ$. By introducing 6% of PVP into the casting dope, its contact angle was reduced to $68.16^\circ \pm 0.37^\circ$ (membrane P2). This could be explained by the trapped PVP had formed an integral part of the membrane matrix, thus reducing surface hydrophobicity [35]. Some researchers also reported that water-soluble polymers like PVP would induce swelling in the membrane, thus increasing surface porosity [34]. The higher surface porosity of the membrane has resulted in a lower static

water contact angle [36,37]. By forming a continuous PDA layer on membrane P3, the hydrophilic groups ($-\text{OH}$ and $-\text{NH}-$) functional groups [15,16] reduced the contact angle to $61.94^\circ \pm 0.59^\circ$. On top of that, the presence of Ag aggregates on membrane P4 further minimized the contact angle to $59.75^\circ \pm 0.55^\circ$. It could be explained that the immobilized Ag particles are having a great affinity towards water molecules while the formation of Ag aggregates would increase surface roughness to facilitate the deposition of water molecules on the membrane [9,13]. Based on Wenzel's model, adding surface roughness would enhance wettability caused by the chemistry of the surface [38], which is the immobilized hydrophilic Ag. On top of that, PDA coating and Ag immobilization would increase total surface energy due to an increase in polar components on the modified membrane surface [13]. As a result, the membrane P4 has demonstrated the lowest static water contact angle.

3.2. Performance Evaluation of Membranes

3.2.1. Filtration performance of fabricated membranes

Table 1 shows the filtration performance of the fabricated membranes. The PWP of a neat PES membrane P1 was recorded at $27.16 \pm 2.27 \text{ L.m}^{-2}.\text{h}^{-1}.\text{bar}^{-1}$ while its HA rejection was reported at $77.81 \pm 1.52\%$. The addition of 6% PVP into membrane P2 has increased its PWP by more than threefold compared to membrane P1. Research has reported that adding PVP would increase membrane porosity and, therefore improve membrane permeability significantly [32,37,39]. This is because the incorporation of hydrophilic PVP would allow more water molecules to be pulled and upheld to the permeate side through membrane pores and thereby increase water permeability [25]. However, the increment of mem-

Table 1. Filtration Performance of the Fabricated Membranes

Membrane	PWP ($L \cdot m^{-2} \cdot h^{-1} \cdot bar^{-1}$)	HA Rejection (%)	FRR (%)
P1	27.16 \pm 2.27	77.81 \pm 1.52	65.72
P2	89.86 \pm 5.64	86.93 \pm 2.13	66.67
P3	25.83 \pm 2.16	92.40 \pm 1.61	79.00
P4	10.66 \pm 0.70	95.14 \pm 0.53	92.17

brane PWP does not compromise membrane rejection performance. The addition of PVP increased the total concentration of the polymer in the dope and yielded the formation of a membrane with uniform pore sizes [40], which can be observed from the FESEM images. Hence, the PVP-added membrane P2 was found better in rejecting HA along with higher permeance than the neat membrane P1.

The oxidation of dopamine monomers has formed a continuous PDA film on membrane P3, significantly reducing water permeability but improving membrane rejection. This is because the PDA nanoaggregates were anchored to the membrane surface via a strong physical bonding (π -interaction) and resulted in pore shrinkage with the *in situ* formation of a thin PDA layer. The membrane P3 has demonstrated slightly higher HA rejection when compared with the PDA-coated polyvinylidene fluoride membrane designed by Saraswathi et al. [14]. Furthermore, the immobilization of silver particles probably blocked surface pores and deteriorated PWP. The Ag^+ ions also caused oxidation of the residual catechol group which facilitated the self-crosslinking of the PDA nanoaggregates. Although flux was negatively affected, the membrane tended to have greater rejection capability, recording HA rejection of $95.14 \pm 0.53\%$. The result bears comparison to the rejection performance reported for Ag/PDA-coated cellulose acetate [41] and also other thin film composite membranes, such as the TiO_2 /Pebax coated PSf+PES [40] and graphene oxide-incorporated 5PES membrane [42].

FRR test was studied to examine the antifouling capability of fabricated membranes. The FRR of the control membrane P1 is reported at 65.72%. By blending 6% of PVP into the dope solution, the fabricated membrane P2 only shows 1% of FRR improvement, which indicates that the pore-forming agent has minimal effect on membrane antifouling properties. Upon PDA coating, the wettability of fabricated membrane P3 improved significantly alongside FRR. It was believed that the hydrophilic surfaces could create a hydrated layer to prevent the adsorption of foulant [29]. Besides, the formation of PDA film on the membrane surface might reduce the pore sizes and lead to the creation of a smoother surface, which improves the antifouling properties of the fabricated membrane. Upon Ag immobilization, the FRR of membrane P4 was further improved to 92.17% owing to enhanced membrane wettability that minimized the interaction between HA foulant and membrane surface. Researchers opined that water might tightly hold in the vicinity of hydrophilic Ag to form a hydrated layer to hinder HA adsorption [40]. Since the HA could only reversibly contact the membrane, the HA fouling could easily be eliminated by washing and therefore could achieve higher FRR. It is worth mentioning that our membrane P4 showed a slightly higher HA rejection than PDA-coated membranes designed by other researchers [43,44]. Besides, the FRR performance of membrane P4 also bears a comparison with other Ag-incorporated membranes

[45] and Ag/PDA-coated membranes [15,20] when applied for BSA removal.

3.2.2. Antibacterial activity of the fabricated membranes

To evaluate the antibacterial activity of the fabricated membranes, the bacterial diffusion inhibition zone test was conducted and the results are shown in Fig. S2. A clear ring with no bacteria growth would confirm the bacteriostatic effect of the fabricated membrane. From the figure, *E. coli* bacteria infected the vicinity of the membrane coupon of P1, P2 and P3. In comparison, a clear ring without bacterial infection was observed around membrane P4, which signifies excellent antibacterial properties possessed by the Ag-immobilized membrane. It was believed that Ag^+ ions had diffused into the agar and inhibited the growth of microbes surrounding membrane P4. Besides, the released Ag^+ ions entered the bacterial cell, bonded to DNA bases and inhibited DNA replication process [21]. This had prevented bacteria from dividing and contributed to a bacteriostatic effect. The inhibition ring diameter was measured at three random spots and averaged to be 22.8 mm, which is slightly larger than 21 mm reported for Ag/polyether ether sulfone membrane [46].

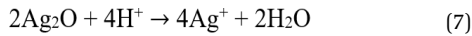
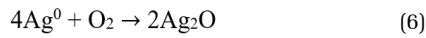
From the SEM images in Fig. 3, bacteria cells infected membranes P1, P2 and P3. It is clearly shown that the pure PES membrane P1 and PVP-added membrane P2 do not exhibit antimicrobial activity. Besides, the viable bacteria cells on membrane P3 also justified that PDA coating did not impart an antibacterial effect. In comparison, the *E. coli* cells were killed and the cell membrane ruptured upon contact with the immobilized Ag on membrane P4. Sile-Yuksel et al. [47] opined that the biocidal capacity of Ag is strongly dependent on the accessibility of bacteria cells to Ag particles. In this experiment, the direct contact between *E. coli* and Ag caused the cell membrane to collapse, followed by cell decomposition and eventually cell death. Ag has interacted with the surface of bacteria cells, allowing the formation of holes and consequent leaking of intracellular contents [48]. Upon comparison, it is evident that membrane P4 shows a bactericidal effect due to Ag incorporation on the PDA-coated membrane.

3.2.3. Long-term stability test of Membrane P4

Silver leaching analysis was performed to examine the stability of the immobilized Ag on membrane P4 for long-term filtration purposes. The concentration of Ag in permeate was determined by using ICP-OES at different time intervals and the results are displayed in Fig. S3. At the beginning of the experiment ($t=0$), the Ag concentration was detected at 0.054 ppm. It was believed that the hydraulic pressure on the membrane might cause the freely-bound Ag to leach out easily during the initial filtration process. The amount of released Ag in permeate was reduced to 0.020 ppm at 6th h and eventually dropped to 0.009 ppm after 12 h of filtration. The leaching of Ag became slow and steady

in the next 36 h by contributing around 0.005 ppm of Ag in the permeate. Such concentration is far below the guideline limit of 0.1 ppm for safe drinking water recommended by the World Health Organization (WHO).

The literature has reported that hydroxyl groups would polymerize and create a strong bonding between PDA and membrane surface [13]. This physical bonding would facilitate a high level of PDA binding on the membrane and minimizes the delamination of the PDA coating. On top of that, catechol groups of PDA show a strong affinity towards Ag. The strong reduction capability of the catechol group would reduce Ag^+ ions, anchor metallic Ag^0 on the membrane surface to improve structural stability [49]. Despite the Ag leaching can be governed by Eqs. (6) and (7), Ag formed via catechol redox chemistry is not sensitive to oxygen and therefore could suppress it from leaching. Long-term stability and safe operation of the Ag/PDA/PES+PVP membrane in a prolonged filtration process can be guaranteed.



3.3. Performance Evaluation of Membrane P4 using Surface Water Samples

3.3.1. Total flux decline

The filtration performance of membrane P4 was examined using water samples collected from Kelana Lake and Klang River. The neat PES membrane P1 is also adopted in this experiment to act as a control and to outline improvements granted by membrane modifications. Table 2 shows the water flux and percentage of TFD of the membranes after filtration. A lower percentage of TFD indicates that the membrane possesses better flux-decline resistance properties [30]. The control membrane P1 exhibited a high percentage of TFD at approximately 50% upon treating surface water samples. In contrast, the membrane P4 shows a much lower flux decline after filtration, probably due to its enhanced membrane wettability. The hydrophilic PDA coating could generate a tightly bound water layer on its surface, for which the repulsive hydration force would prevent the adsorption of hydrophobic foulants in the water sample [50]. This reduced the likelihood of membrane fouling thus rendered a steady flux during membrane filtration. Nevertheless, the immobilized Ag disinfected microorganisms on the membrane surface, suppressing the formation of biofilm and

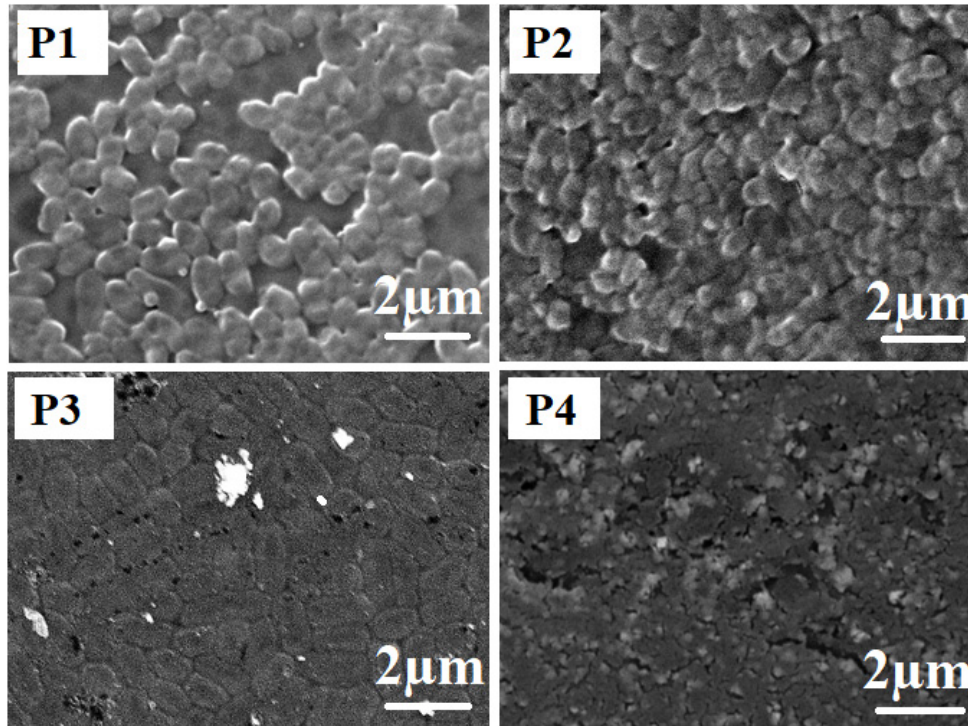


Fig. 3. SEM observation of incubated bacteria on membranes.

Table 2. Membranes Water Flux and TFD upon Treating Surface Water Samples

Membrane	Pure Water Flux ($\text{L}\cdot\text{m}^{-2}\cdot\text{h}^{-1}$)	Lake Water		River Water	
		Permeate Flux ($\text{L}\cdot\text{m}^{-2}\cdot\text{h}^{-1}$)	TFD (%)	Permeate Flux ($\text{L}\cdot\text{m}^{-2}\cdot\text{h}^{-1}$)	TFD (%)
P1	27.16 ± 2.27	13.15 ± 1.76	51.59	13.67 ± 1.79	49.67
P4	10.66 ± 0.70	9.03 ± 0.45	15.26	8.71 ± 0.54	18.34

Table 3. Water Quality Assessment for Lake Water

Parameters	P1 (Neat PES)		P4 (Ag/PDA/PES+PVP)	
	Permeate (mg/L)	Removal (%)	Permeate (mg/L)	Removal (%)
TSS (Feed = 74.0 mg/L)	43.90 ± 1.75	40.68 ± 2.37	36.77 ± 2.21	50.32 ± 2.99
Turbidity (Feed = 31.8 NTU)	2.80 ± 0.19 NTU	91.18 ± 0.59 NTU	0.75 ± 0.29 NTU	97.63 ± 0.93NTU
COD (Feed = 66 mg/L)	21.33 ± 3.21	67.67 ± 4.87	14.0 ± 1.00	78.79 ± 1.52
TDS (Feed = 103.74 mg/L)	86.01 ± 4.12	17.09 ± 3.97	75.88 ± 4.96	26.86 ± 4.78
pH (Feed = 5.04)	5.75 ± 0.04		6.34 ± 0.06	

Table 4. Water Quality Assessment for River Water

Parameters	P1 (Neat PES)		P4 (Ag/PDA/PES+PVP)	
	Permeate (mg/L)	Removal (%)	Permeate (mg/L)	Removal (%)
TSS (Feed = 71.5 mg/L)	27.17 ± 0.86	62.00 ± 1.20	19.80 ± 1.67	72.31 ± 2.34
Turbidity (Feed = 70.0 NTU)	3.05 ± 0.78 NTU	95.63 ± 1.11 NTU	0.99 ± 0.45 NTU	98.58 ± 0.63NTU
COD (Feed = 22 mg/L)	15.67 ± 1.53	28.79 ± 6.94	7.67 ± 0.58	65.15 ± 2.62
TDS (Feed = 94.12 mg/L)	73.12 ± 2.05	22.32 ± 2.17	65.44 ± 3.69	30.47 ± 3.92
pH (Feed = 5.68)	5.76 ± 0.23		6.46 ± 0.04	

mitigating biofouling [48].

3.3.2. Water samples quality assessment

Tables 3 and 4 show the water parameters of Kelana Lake and Klang River water samples along with the quality of permeate produced by control membrane P1 and modified membrane P4. In general, membrane P4 shows higher TSS, turbidity, COD and TDS removal than membrane P1. Higher contaminant removal could be attributed to several reasons. From Fig. 2, the addition of PVP significantly minimized pore size distribution and suppressed the formation of huge pores. The formation of continuous PDA film covered up membrane pores and resulted in pore shrinkage [9]. During Ag immobilization, Ag⁺ ions also triggered self-crosslinking of the PDA nanoaggregates in the PDA layer and further improved membrane rejection performance.

As TSS are suspended particulates with size > 0.45 µm, membrane P4 with a more even pore size distribution could improve the TSS removal rate by 10% for both surface water samples compared to membrane P1. For turbidity investigation, the initial values of lake and river water were reported to be 31.8 NTU and 70 NTU, respectively. This shows that river water contained more suspended and dissolved particles (e.g., organic matter, algae and microscopic organisms) than lake water, which scattered light and turned water cloudy. Upon filtration, lake and river water permeates released from both membranes P1 and P4 achieved more than 90% of turbidity removal. It is worth mentioning that the turbidity of the permeate generated by membrane P4 is similar to the turbidity value of a tap water sample in Kuala Lumpur, which is 0.86 NTU [51]. The superior performance could be attributed to the PDA coating that covered up membrane pores and enhanced particulates rejection by molecular sieving.

The initial COD of lake water feed was much higher than river water probably due to the presence of high algae content as observed in the greenish lake water sample. Upon filtration, high COD removal was achieved by both membranes in treating lake water since the suspended algae could be easily removed by molecular sieving. In contrast, the COD removal from river water by membrane

P4 was much higher than by membrane P1. It was believed that the PDA coating and Ag immobilization improved the separation efficiency of the membrane to retain more organic matter that caused COD in river water. From the tables, both membranes achieved a fair result in removing TDS from surface water samples. This was a norm as TDS was mainly composed of dissolved ions [52] which is not favourable to be removed by the PES membrane, similar to the literature that reported 23.5% of NaCl rejection using PES membrane [53]. Comparing membrane P1, membrane P4 shows higher TDS removal from the lake and river water samples by approximately 10% and 8%, respectively. This could be due to the blocked pores in membrane P4 that improved solute rejection.

The measured pHs of the lake and river water samples were 5.04 and 5.68, respectively. A pond with a pH value less than 6 might result in a stunted, reduced or even absence of fish population, which greatly affects the ecosystem. Upon filtration, the pH value of lake water permeates produced by the membrane P1 was changed from 5.04 to 5.75. The increment was much more significant after utilizing membrane P4 where the permeate pH value was increased from 5.68 to 6.34. Similarly, the pH values of river water also increased to 5.76 and 6.46 upon filtration using control membrane P1 and membrane P4, respectively. This shows that acidic pollutants have been effectively removed by the membrane P4 owing to the coating of PDA and Ag immobilization.

3.3.3. Removal of bacterial from Klang River and Kelana Lake water by filtration

The bacterial removal performance of neat PES membrane (P1) and modified Ag/PDA/PES membrane (P4) were compared. A dilution factor of 10 was applied for both lake and river water samples before incubation. The results are illustrated in Fig. 4. It can be seen that bacteria colonies presented in lake and river water feed were unquantifiable. Upon filtration using the control P1 membrane, the bacteria colonies were slightly reduced but still considered too numerous to count (>300 colonies per plate). Low bacteria rejection was probably due to the presence of extraordinarily huge pores which significantly deteriorated the molecular sieving effect

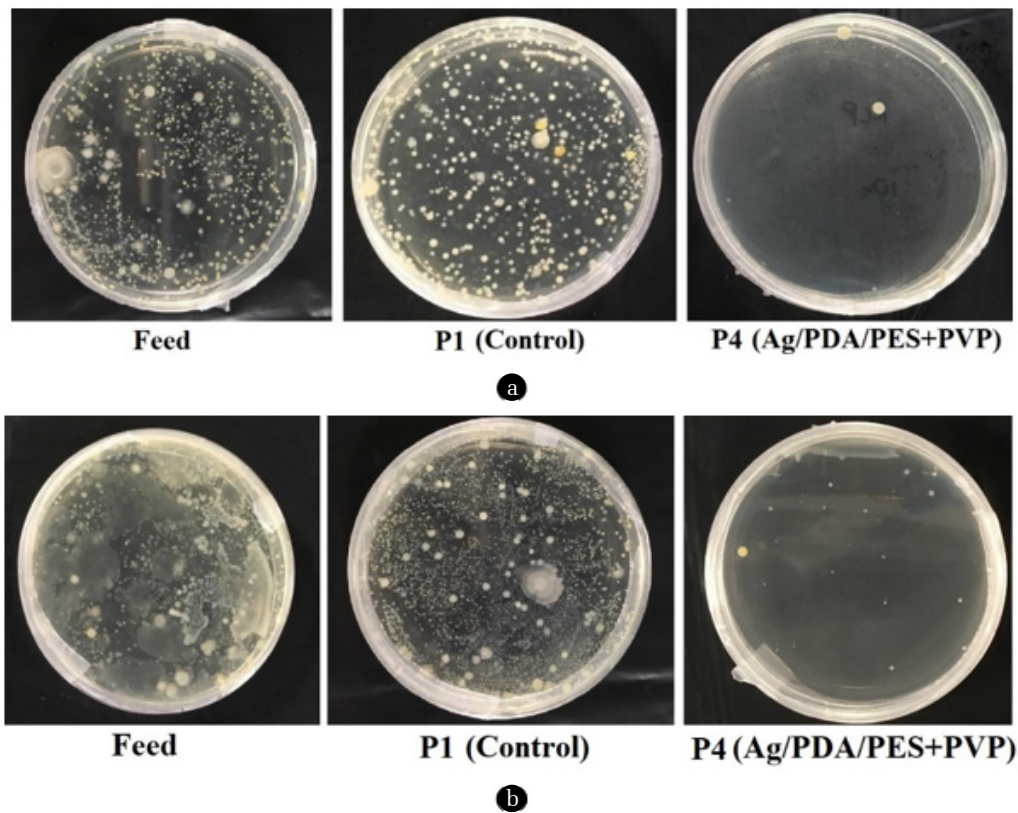


Fig. 4. Bacteria content in (a) Kelana Lake water sample and (b) Klang River water sample.

of membrane P1. In contrast, only 4 colonies formed on the agar plate containing lake water permeate produced by modified membrane P4. Approximately 25 colonies were observed in the river water permeate for modified membrane P4. It should be noted that the colonies presented in both permeate were considered too few to count (<30 colonies per plate).

From this experiment, the modified membrane P4 (Ag/PDA/PES+PVP) possessed excellent bacterial removal performance over membrane P1 (neat PES). The immobilized Ag and the leached Ag⁺ are a non-specific antibacterial agent that acts against a wide range of microorganism upon contact [15]. However, complete elimination of microbes is not possible because Ag might not be accessible to certain bacterial cells [54]. Furthermore, the working environment where permeate was collected might have microorganisms contamination, which is generally unavoidable.

4. Conclusions

In this study, four membrane samples were produced, namely PES (P1), PES+PVP (P2), PDA/PES+PVP (P3) and Ag/PDA/PES+PVP (P4) membranes. All samples were characterized using SEM, FESEM, EDX and contact angle goniometer to investigate the cross-sectional morphology, surface morphology, elemental composition as well as the wettability of the membranes. For the HA rejection test conducted at 1 bar, the pure PES membrane (P1)

removed 77.81% of HA with 65.72% of FRR. Incorporation of 6% PVP into membrane P2 improved HA rejection to 86.93% but showed minimal effect on membrane antifouling properties. In contrast, the PDA coating on membrane P3 significantly improved HA rejection and FRR to 92.40% and 79.00%, respectively. Upon Ag immobilization, the HA rejection was enhanced to 95.14% while FRR was improved to 92.17%. Nevertheless, the membrane P4 (Ag/PDA/PES+PVP) demonstrated excellent bacteriostatic and bactericidal capability in the antibacterial activity tests. The catechol groups in PDA strongly anchored Ag to minimize its leaching, thus the amount of Ag detected in the permeate throughout the filtration process was maintained below the maximum Ag contamination limit of 0.1 ppm in drinking water affixed by WHO. The membrane P4 also showed higher contaminant removal (TSS, turbidity, COD and TDS) and lower TFD as compared to control membrane P1 in treating surface water samples. Last but not least, the membrane P4 demonstrated excellent bacterial removal performance to justify its practical application in treating bacteria-contaminated surface water samples.

Acknowledgments

The authors wish to express their gratitude to Universiti Tunku Abdul Rahman (UTAR) for providing financial support through UTARRF under Project No: IPSR/RMC/UTARRF/2016-C1/K2.

Conflict-of-interest

The authors declare that they have no conflict of interest.

Author contributions

K.P.W. (Postgraduate Student) carried out the experiments, data analysis, interpretation and wrote the original draft. C.H.K. (Associate Professor) conceptualised and supervised the project, acquired funding, provided resources for the experiments and contributed to the final revision of the manuscript. Y.L.P. (Associate Professor) and W.J.L. (Associate Professor) co-supervised the student and reviewed the written manuscript. W.C.C. (Assistant Professor) advised on the design of the experiment and provided instrumentations during the experimental stage works.

Nomenclature

Ag	Silver
BSA	Bovine serum albumin
CFU	Colony-forming unit
COD	chemical oxygen demand
C_p	HA concentration of permeate
C_f	HA concentration of feed
EDX	Energy-dispersive X-ray analysis
FESEM	Field emission scanning electron microscope
FRR	Flux recovery rate
HA	Humic acid
ICP-OES	Inductively coupled plasma-optical emission spectrometry
MF	Microfiltration
NOMs	Natural organic matters
PAN	Polyacrylonitrile
PDA	Polydopamine
PEI	Poly(ether imide)
PES	Polyethersulfone
PVP	Polyvinylpyrrolidone
PWP	pure water permeability
RO	Reverse osmosis
R_{HA}	HA rejection percentage
SEM	Scanning electron microscope
TDS	total dissolved solids
TSS	total suspended solids
UF	Ultrafiltration
J_{w1}	initial water flux
J_{w2}	water flux of the regenerated membrane

References

- Lee KT, Wai KP, Lu SY. CuO nanorods from carrier solvent assisted interfacial reaction processes: An unexpected extraordinary Fe-free photocatalyst in sunlight assisted Fenton-like processes. *J. Taiwan Inst. Chem. Eng.* 2017;70:244–251. <https://doi.org/10.1016/j.jtice.2016.10.057>.
- Song JJ, Huang Y, Nam SW et al. Ultrathin graphene oxide membranes for the removal of humic acid. *Sep. Purif. Technol.* 2015;144:162–167. <https://doi.org/10.1016/j.seppur.2015.02.032>.
- Koo CH, Mohammad AW, Suja F. Effect of cross-flow velocity on membrane filtration performance in relation to membrane properties. *Desalin. Water Treat.* 2015;55:678–692. <https://doi.org/10.1080/19443994.2014.953594>.
- Mohammadi MJ, Salari J, Takdastan A et al. Removal of turbidity and organic matter from car wash wastewater by electro-coagulation process. *Desalin. Water Treat.* 2017;68:122–128. <https://doi.org/10.5004/dwt.2017.20319>.
- Menya E, Olupot PW, Storz H, Lubwama M, Kiros Y. Production and performance of activated carbon from rice husks for removal of natural organic matter from water: A review. *Chem. Eng. Res. Des.* 2018;129:271–296. <https://doi.org/10.1016/j.cherd.2017.11.008>.
- Gora SL, Andrews SA. Removal of natural organic matter and disinfection byproduct precursors from drinking water using photocatalytically regenerable nanoscale adsorbents. *Chemosphere* 2019;218:52–63. <https://doi.org/10.1016/j.chemosphere.2018.11.102>.
- Castro-Muñoz R, Yáñez-Fernández J, Fíla V. Phenolic compounds recovered from agro-food by-products using membrane technologies: An overview. *Food Chem.* 2016;213:753–762. <https://doi.org/10.1016/j.foodchem.2016.07.030>.
- Ahmad AL, Abdulkarim AA, Ismail S, Ooi BS. Preparation and characterisation of PES-ZnO mixed matrix membranes for humic acid removal. *Desalin. Water Treat.* 2015;54:3257–3268. <https://doi.org/10.1080/19443994.2014.910137>.
- Zhang R, Su Y, Zhou L et al. Manipulating the multifunctionalities of polydopamine to prepare high-flux anti-biofouling composite nanofiltration membranes. *RSC Adv.* 2016;6:32863–32873. <https://doi.org/10.1039/C6RA04458A>.
- Thuyavan YL, Anantharaman N, Arthanareeswaran G, Ismail AF. Impact of solvents and process conditions on the formation of polyethersulfone membranes and its fouling behavior in lake water filtration. *J. Chem. Technol. Biotechnol.* 2016;91:2568–2581. <https://doi.org/10.1002/jctb.4846>.
- Biswas P, Bandyopadhyaya R. Biofouling prevention using silver nanoparticle impregnated polyethersulfone (PES) membrane: E. coli cell-killing in a continuous cross-flow membrane module. *J. Colloid Interface Sci.* 2017;491:13–26. <https://doi.org/10.1016/j.jcis.2016.11.060>.
- Wai KP, Koo CH, Pang YL, Chong WC, Lau WJ. In situ immobilization of silver on polydopamine-coated composite membrane for enhanced antibacterial properties. *J. Water Process Eng.* 2020;33:100989. <https://doi.org/10.1016/j.jwpe.2019.100989>.
- Saraswathi M, Rana D, Alwarappan S et al. Polydopamine layered poly (ether imide) ultrafiltration membranes tailored with silver nanoparticles designed for better permeability, se-

- lectivity and antifouling. *J. Ind. Eng. Chem.* 2019;76:141–149. <https://doi.org/10.1016/j.jiec.2019.03.014>.
14. Saraswathi M, Kausalya R, Kaleekkal NJ, Rana D, Nagendran A. BSA and humic acid separation from aqueous stream using polydopamine coated PVDF ultrafiltration membranes. *J. Environ. Chem. Eng.* 2017;5:2937–2943. <https://doi.org/10.1016/j.jece.2017.05.051>.
 15. Huang L, Zhao S, Wang Z et al. In situ immobilization of silver nanoparticles for improving permeability, antifouling and anti-bacterial properties of ultrafiltration membrane. *J. Memb. Sci.* 2016;499:269–281. <https://doi.org/10.1016/j.memsci.2015.10.055>.
 16. Yang E, Chae KJ, Alayande AB, Kim KY, Kim IS. Concurrent performance improvement and biofouling mitigation in osmotic microbial fuel cells using a silver nanoparticle-polydopamine coated forward osmosis membrane. *J. Memb. Sci.* 2016;513:217–225. <https://doi.org/10.1016/j.memsci.2016.04.028>.
 17. Zodrow K, Brunet L, Mahendra S et al. Polysulfone ultrafiltration membranes impregnated with silver nanoparticles show improved biofouling resistance and virus removal. *Water Res.* 2009;43:715–723. <https://doi.org/10.1016/j.watres.2008.11.014>.
 18. Xiu Z, Zhang Q, Puppala HL, Colvin VL, Alvarez PJJ. Negligible Particle-Specific Antibacterial Activity of Silver Nanoparticles. *Nano Lett.* 2012;12:4271–4275. <https://doi.org/10.1021/nl301934w>.
 19. Li W-R, Xie XB, Shi QS et al. Antibacterial activity and mechanism of silver nanoparticles on Escherichia coli. *Appl. Microbiol. Biotechnol.* 2010;85:1115–1122. <https://doi.org/10.1007/s00253-009-2159-5>.
 20. Saraswathi MS, Rana D, Alwarappan S et al. Cellulose acetate ultrafiltration membranes customized with bio-inspired polydopamine coating and in situ immobilization of silver nanoparticles. *New J. Chem.* 2019;43:4216–4225. <https://doi.org/10.1039/C8NJ04511A>.
 21. Guo L, Yuan W, Lu Z, Li CM. Polymer/nanosilver composite coatings for antibacterial applications. *Colloids Surfaces A Physicochem. Eng. Asp.* 2013;439:69–83. <https://doi.org/10.1016/j.colsurfa.2012.12.029>.
 22. Wang J, Wu Y, Yang Z et al. A novel gravity-driven nanofibrous membrane for point-of-use water disinfection: polydopamine-induced in situ silver incorporation. *Sci. Rep.* 2017; 7:2334. <https://doi.org/10.1038/s41598-017-02452-2>.
 23. GhavamiNejad A, Unnithan RA, Sasikala RKA et al. Mussel-Inspired Electrospun Nanofibers Functionalized with Size-Controlled Silver Nanoparticles for Wound Dressing Application. *ACS Appl. Mater. Interfaces* 2015;7:12176–12183. <https://doi.org/10.1021/acsami.5b02542>.
 24. Cai R, Tao G, He H et al. One-step synthesis of silver nanoparticles on polydopamine-coated sericin/polyvinyl alcohol composite films for potential antimicrobial applications. *Molecules* 2017;22:721. <https://doi.org/10.3390/molecules22050721>.
 25. Ananth A, Arthanareeswaran G, Ismail A, Mok YS, Matsuura T. Effect of bio-mediated route synthesized silver nanoparticles for modification of polyethersulfone membranes. *Colloids Surfaces A Physicochem. Eng. Asp.* 2014;451:151–160. <https://doi.org/10.1016/j.colsurfa.2014.03.024>.
 26. Gohari JR, Lau WJ, Matsuura T, Ismail AF. Effect of surface pattern formation on membrane fouling and its control in phase inversion process. *J. Memb. Sci.* 2013;446:326–331. <https://doi.org/10.1016/j.memsci.2013.06.056>.
 27. Panda SR, Mukherjee M, De S. Preparation, characterization and humic acid removal capacity of chitosan coated iron-oxide-polyacrylonitrile mixed matrix membrane. *J. Water Process Eng.* 2015;6:93–104. <https://doi.org/10.1016/j.jwpe.2015.03.007>.
 28. Wang J, Lang WZ, Xu HP, Zhang X, Guo YJ. Improved poly(vinyl butyral) hollow fiber membranes by embedding multi-walled carbon nanotube for the ultrafiltrations of bovine serum albumin and humic acid. *Chem. Eng. J.* 2015;260:90–98. <https://doi.org/10.1016/j.cej.2014.08.082>.
 29. Kumar M, Gholamvand Z, Morrissey A et al. Preparation and characterization of low fouling novel hybrid ultrafiltration membranes based on the blends of GO–TiO₂ nanocomposite and polysulfone for humic acid removal. *J. Memb. Sci.* 2016;506:38–49. <https://doi.org/10.1016/j.memsci.2016.02.005>.
 30. Chen W, Su Y, Peng J et al. Engineering a Robust, Versatile amphiphilic membrane surface through forced surface segregation for ultralow flux-decline. *Adv. Funct. Mater.* 2011;21:191–198. <https://doi.org/10.1002/adfm.201001384>.
 31. Chong WC, Mahmoudi E, Chung YT et al. Polyvinylidene fluoride membranes with enhanced antibacterial and low fouling properties by incorporating ZnO/rGO composites. *Desalination Water Treat.* 2017;96:12–21. <https://doi.org/10.5004/dwt.2017.20742>.
 32. Sun Z, Chen F. Hydrophilicity and antifouling property of membrane materials from cellulose acetate/polyethersulfone in DMAc. *Int. J. Biol. Macromol.* 2016;91:143–150. <https://doi.org/10.1016/j.ijbiomac.2016.05.072>.
 33. Wan L-S, Xu ZK, Wang ZG. Leaching of PVP from polyacrylonitrile/PVP blending membranes: A comparative study of asymmetric and dense membranes. *J. Polym. Sci. Part B Polym. Phys.* 2006;44:1490–1498. <https://doi.org/10.1002/polb.20804>.
 34. Basri H, Ismail AF, Aziz M. Polyethersulfone (PES)–silver composite UF membrane: Effect of silver loading and PVP molecular weight on membrane morphology and antibacterial activity. *Desalination* 2011;273:72–80. <https://doi.org/10.1016/j.desal.2010.11.010>.
 35. Vatsha B, Ngila JC, Moutloali RM. Preparation of antifouling polyvinylpyrrolidone (PVP 40K) modified polyethersulfone (PES) ultrafiltration (UF) membrane for water purification. *Phys. Chem. Earth, Parts A/B/C* 2014;67–69:125–131. <https://doi.org/10.1016/j.pce.2013.09.021>.
 36. Rana D, Matsuura T. Surface modifications for antifouling membranes. *Chem. Rev.* 2010;110:2448–2471. <https://doi.org/10.1021/cr800208y>.
 37. Omidvar M, Soltanieh M, Mousavi SM et al. Preparation of hydrophilic nanofiltration membranes for removal of pharmaceuticals from water. *J. Environ. Heal. Sci. Eng.* 2015;13:42. <https://doi.org/10.1186/s40201-015-0201-3>.
 38. Wenzel RN. Resistance of solid surfaces to wetting by water. *Ind. Eng. Chem.* 1936;28:988–994. <https://doi.org/10.1021/ie50320a024>.
 39. Basri H, Ismail AF, Aziz M et al. Silver-filled polyethersulfone membranes for antibacterial applications — Effect of PVP and

- TAP addition on silver dispersion. *Desalination* 2010;261:264–271. <https://doi.org/10.1016/j.desal.2010.05.009>.
40. Cheshomi N, Pakizeh M, Namvar-Mahboub M. Preparation and characterization of TiO₂/Pebax/(PSf-PES) thin film nanocomposite membrane for humic acid removal from water. *Polym. Adv. Technol.* 2018;29:1303–1312. <https://doi.org/10.1002/pat.4242>.
 41. Saraswathi M, Mahalakshmi S, Vetrivel S et al. Separation of bovine serum albumin and humic acid contaminants from aqueous stream using tailored poly (amide imide) ultrafiltration membranes. *J. Environ. Chem. Eng.* 2018;6:1912–1917. <https://doi.org/10.1016/j.jece.2018.02.036>.
 42. Algamdi MS, Alsohaimi IH, Lawler J et al. Fabrication of graphene oxide incorporated polyethersulfone hybrid ultrafiltration membranes for humic acid removal. *Sep. Purif. Technol.* 2019;223:17–23. <https://doi.org/10.1016/j.seppur.2019.04.057>.
 43. Li Y, Su Y, Zhao X et al. Antifouling, high-flux nanofiltration membranes enabled by dual functional polydopamine. *ACS Appl. Mater. Interfaces* 2014;6:5548–5557. <https://doi.org/10.1021/am405990g>.
 44. Saraswathi MSA, Kausalya R, Kaleekkal NJ, Rana D, Nagendran A. BSA and humic acid separation from aqueous stream using polydopamine coated PVDF ultrafiltration membranes. *J. Environ. Chem. Eng.* 2017;5:2937–2943. <https://doi.org/10.1016/j.jece.2017.05.051>.
 45. Mollahosseini A, Rahimpour A, Jahamshahi M, Peyravi M, Khavarpour M. The effect of silver nanoparticle size on performance and antibacteriability of polysulfone ultrafiltration membrane. *Desalination* 2012;306:41–50. <https://doi.org/10.1016/j.desal.2012.08.035>.
 46. Maheswari P, Prasannadevi D, Mohan D. Preparation and performance of silver nanoparticle incorporated polyethersulfone nanofiltration membranes. *High Perform. Polym.* 2013;25:174–187. <https://doi.org/10.1177/0954008312459865>.
 47. Sile-Yuksel M, Tas B, Koseoglu-Imer DY, Koyuncu I. Effect of silver nanoparticle (AgNP) location in nanocomposite membrane matrix fabricated with different polymer type on antibacterial mechanism. *Desalination* 2014;347:120–130. <https://doi.org/10.1016/j.desal.2014.05.022>.
 48. Andrade PF, de Faria AF, Quites FJ et al. Inhibition of bacterial adhesion on cellulose acetate membranes containing silver nanoparticles. *Cellulose* 2015;22:3895–3906. <https://doi.org/10.1007/s10570-015-0752-6>.
 49. GhavamiNejad A, Aguilar LE, Ambade RB et al. Immobilization of silver nanoparticles on electropolymerized polydopamine films for metal implant applications. *Colloids Interface Sci. Commun.* 2015;6:5–8. <https://doi.org/10.1016/j.colcom.2015.08.001>.
 50. Jiang BB, Sun XF, Wang L et al. Polyethersulfone membranes modified with D-tyrosine for biofouling mitigation: Synergistic effect of surface hydrophility and anti-microbial properties. *Chem. Eng. J.* 2017;311:135–142. <https://doi.org/10.1016/j.cej.2016.11.088>.
 51. Ong C, Ibrahim S, Gupta BS. A survey of tap water quality in Kuala Lumpur. *Urban Water J.* 2007;4:29–41. <https://doi.org/10.1080/15730620601145923>.
 52. Zhang C, Zhang W, Huang Y, Gao X. Analysing the correlations of long-term seasonal water quality parameters, suspended solids and total dissolved solids in a shallow reservoir with meteorological factors. *Environ. Sci. Pollut. Res.* 2017;24:6746–6756. <https://doi.org/10.1007/s11356-017-8402-1>.
 53. Nora'aini A, Mohammad AW, Jusoh A et al. Treatment of aquaculture wastewater using ultra-low pressure asymmetric polyethersulfone (PES) membrane. *Desal.* 2005;185:317–326. <https://doi.org/10.1016/j.desal.2005.03.084>.
 54. Dolina J, Dlask O, Lederer T, Dvořák L. Mitigation of membrane biofouling through surface modification with different forms of nanosilver. *Chem. Eng. J.* 2015;275:125–133. <https://doi.org/10.1016/j.cej.2015.04.008>.